Quantum Optics with Nanocrystal Quantum Dots in Solution: Quantitative Study of Clustering

David A. Bussian,[†] Anton V. Malko,[‡] Han Htoon,[†] Yongfen Chen,[†] Jennifer A. Hollingsworth,[†] and Victor I. Klimov*,[†]

Chemistry Division and Center for Integrated Nanotechnologies, Los Alamos National Laboratory, Los Alamos, New Mexico 87545, and Department of Physics, University of Texas at Dallas, Richardson, Texas 75080

Received: July 14, 2008; Revised Manuscript Received: November 17, 2008

Applying a combination of traditional fluorescence correlation spectroscopy and antibunching measurements to solutions of nanocrystal quantum dots (NQDs), we can reliably establish the regime where only one dot or less is present in the detection volume. Under these conditions, it is possible to probe various photophysical properties of colloidal nanocrystals with single-dot sensitivity in their "native" solution environment. We apply this method to quantitative studies of NQD aggregation. By first measuring dilute Rhodamine 590 solutions that have no aggregation, we find that the clustering parameter, $\langle n \rangle$ (the average number of quantum emitters per diffusing cluster), can be determined with better than 5% accuracy. We then use this technique to quantify clustering of CdSe NQDs prepared either as toluene or aqueous solutions. On the basis of the correlation data, NQDs exhibit minimal aggregation ($\langle n \rangle$ is less than 1.1−1.2) in fresh as-prepared solutions for both aqueous and nonaqueous systems. On the other hand, sample aging leads to considerable increase in the degree of aggregation as indicated by increased values of $\langle n \rangle$. For example, in a sample of biotinylated NQDs aged for 120 days the number of two-dot aggregates becomes approximately equal to that of isolated NQDs. The ability to study single dots in solutions, demonstrated here, opens interesting opportunities for both biorelated research and also for studies of fundamental photophysics of nanocrystals, especially the effects of environment on electronic structures and carrier relaxation behaviors.

1. Introduction

Semiconductor nanocrystal quantum dots (NQDs) are promising materials for applications in light-emitting technologies such as NQD lasers,[1,2] light emitting diodes,[3,4] and biolabeling.[5−7] The common description of NQDs is that of isolated nanocrystalline cores surrounded by organic ligand molecules that provide electronic passivation of the surface, prevent aggregation, and render NQDs soluble. Generally synthesized in organic solutions using amphiphilic ligands such as trioctylphosphine (TOP) and trioctylphosphine oxide (TOPO), NQDs can be fabricated with a high degree of monodispersity and emission quantum yields approaching 100%.[8−10] NQDs have been the focus of numerous studies to understand the effects of quantum confinement on their optical and electronic properties.[11] In recent years, chemists have developed a variety of methods for producing stable, water-soluble, biocompatible NQDs.[5,7,12,13] These advances have initiated a burgeoning effort in the development of NQD-based biological labels that take advantage of high brightness, good photostability, and narrow, spectrally tunable emission lines of colloidal nanocrystals.

Many important insights into light-emitting properties of NQDs have been provided by single-dot studies, which allow one to obtain information on the structure of emitting states, photoluminescence (PL) polarization characteristics, and decay dynamics without complications associated with ensemble averaging.[14−16] Most of the single-dot experiments have been conducted on dilute NQD assemblies prepared in the form of solid-state films. It is, however, not obvious that the results of these studies can be applied to samples in solution forms because light-emission properties of individual NQDs are known to exhibit extreme sensitivity to their environment and, hence, are expected to differ significantly for solid-state and solution samples.

Recently, several approaches have been applied to study single NQDs in solution. One such attempt utilized surface-immobilized CdSe/ZnS NQDs in conjunction with scanning confocal microscopy.[17] A potential drawback of this approach is, however, the use of special immobilization chemistry that may impact NQD properties. Recently, fluorescence correlation spectroscopy (FCS) has been shown to be a viable alternative to scanning microscopy approaches.[18] In addition to providing single particle sensitivity it allows for rapid data collection unattainable with current scanning methods.[19]

FCS uses a small submicron illumination volume to excite diffusing chromophores in solution and to collect the temporally resolved fluorescence. By correlating the "flashes" of luminescence that occur when a chromophore passes through the excitation volume, FCS yields information on processes that cause fluctuation of the collected signal. Traditionally, FCS has been used to quantify fluctuations on time scales comparable to the chromophore diffusion time, τ_D, which is typically on the order of microseconds. In the case of NQDs, information on the hydrodynamic radius, the average particle number in the excitation volume, and blinking statistics[18,20] can be obtained.

One drawback of traditional FCS is that by analyzing the signals on long (microsecond) time scales, relevant to diffusion, one cannot distinguish between single diffusing emitters and aggregates that comprise several emitting species, as is the case of multiply labeled biomolecules or aggregated NQDs. On the

* To whom correspondence should be addressed. E-mail: klimov@lanl.gov.
[†] Los Alamos National Laboratory.
[‡] University of Texas at Dallas.

10.1021/jp806219s CCC: $40.75
Published on Web 01/20/2009

other hand, the ability to make a distinction between these two types of emitters is very important in studies that exploit the quantum-mechanical nature of emitting species.

To determine the number of emitters per diffusing cluster, one can measure the intensity autocorrelation function on short times, of the order of the radiative lifetime, $\tau_R = 1/\Gamma$. Since it takes a nonzero time for a quantum-mechanical system to cycle between the ground and excited states, the probability of detecting two sequential photons decreases with decreasing delay time, which is known as fluorescence antibunching. This effect leads to an "anticorrelation dip" in the intensity autocorrelation function at zero time with the amplitude, providing a direct measure of the number of quantum emitters present in the detection volume. Thus, by conducting both antibunching measurements and traditional FCS, one can potentially quantify the number of chromophores per cluster (clustering parameter) together with the number of diffusing particles in the detection volume (occupation factor).

Recently, McHale et al. used a single particle tracking technique to observe antibunching in PL from single NQDs in solution.[21] In another study conducted by Sykora et al.,[22] the combination of antibunching and FCS measurements was applied to quantify the stoichiometry of biological complexes labeled with a fixed number of molecular dyes. Here, we demonstrate the utility of these two techniques for addressing an important issue, aggregation of NQDs in solution. Depending on the NQD surface chemistry and sample preparation, we observe a wide variety of aggregation behaviors from well-isolated single dots to significant clustering of dots. By allowing one to clearly establish the regime in which one interrogates properties of individual dots but not dot aggregates, the reported technique opens interesting opportunities for studies of photophysics of single NQDs in their "native" solution environment.

2. Materials and Methods

Samples. Sub-nanomolar concentrations of Rhodamine 590 (Rh590) solutions were prepared in distilled and deionized water and were used as reference samples in autocorrelation studies. Since dye molecules do not have a tendency to aggregate (particularly at the high dilutions used in these experiments), the expected value of the clustering parameter for them is 1.

Water-soluble, biotinylated NQDs emitting at 655 nm were purchased from Invitrogen Corp. "Standard" hydrophobic NQDs passivated with octylamine molecules with emission at 620 nm were synthesized using a multishell approach adapted from a previous study[23] (see insets in Figure 1 for arrangement of various shell layers). Figure 1 shows typical absorption and PL spectra of (a) organic-soluble and (b) water-soluble NQDs. Samples for photon correlation studies were prepared by loading 30 μL of an NQD solution into a sealed cell made of two glass coverslips held together by an adhesive spacer layer (Grace Bio-Laboratories, Inc.); the cell thickness was 120 μm.

Since typical antibunching measurements require fairly high emission rates (greater than 10 kHz per channel), we use only highly emissive NQD samples with PL quantum yields greater than 50% in our experiments. For these high-quality NQDs, we did not observe significant variations in measured photon-correlation data between samples with nominally identical surface passivation.

Experimental Setup. Intensity correlation data were acquired using a standard epi-fluorescence confocal setup based on an Olympus IX 70 inverted microscope. The output of a continuous-wave (cw) 532 nm Nd:YAG diode-pumped solid-state laser was spatially filtered through a 25 μm pinhole and sent into a

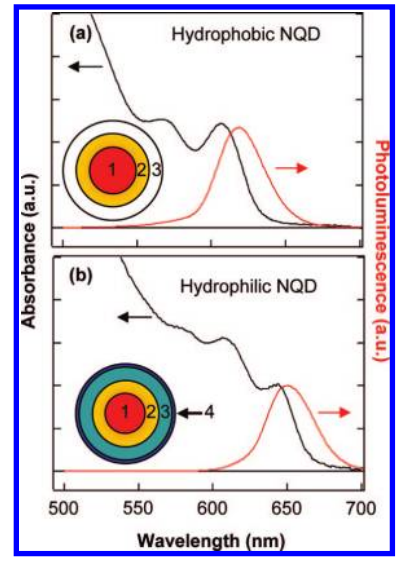

Figure 1. Examples of absorption (black line) and PL (red line) spectra of hydrophobic (a) and hydrophilic (b) NQDs with insets illustrating the structure of these dots. Hydrophobic NQDs are composed of CdSe(1)/CdS/ZnS(2)/octylamine(3), and hydrophilic NQDs are composed of CdSe(1)/ZnS(2)/polymer(3)/biotin(4).

60×, 1.2 numerical aperture water-immersion objective (Olympus) producing an excitation volume of ca. 1 fL. Fluorescence collected by the same objective was directed through a dichroic mirror onto a 70-μm pinhole, and residual laser light was subsequently removed with either a long-pass or a band-pass interference filter. The PL signal was then split by a 50/50 nonpolarizing beam splitter and directed onto the active areas of two single photon counting avalanche photodiodes (APDs) (Perkin-Elmer, SPCM, AQR-14). The pulses from the APDs were simultaneously sent to the start and the stop channels of a time-correlated-single-photon-counting card (Becker & Hickl, SPC-630) for antibunching measurements using a standard Hanbury-Brown-Twiss setup and to an autocorrelator for measuring long-time FCS (ALV-GmBH, ALV6000).

Despite the fact that they are often implemented independently and in different environments, both FCS and antibunching measurements provide information on the same quantity - the intensity autocorrelation function (see below), however, on different time scales. FCS allows one to analyze longer timescales characteristic of, for example, particle diffusion, while antibunching measurements are applied on shorter timescales defined by the radiative lifetime of chromophores under investigation.[24] The necessity for two detectors in the antibunching configuration stems from the fact that commonly used APDs have a significant "dead" time (~50 ns), which precludes using them to measure simultaneous photon pairs.

Data Analysis. The quantity which is analyzed in our measurements is the PL intensity (I) autocorrelation function, $g^{(2)}(\tau)$, defined as

$$g^{(2)}(\tau) = \frac{\langle I(t)I(t+\tau)\rangle}{\langle I(t)\rangle^2} \quad (1)$$

where the brackets denote an average over time t, from nanoseconds to milliseconds. The form of the second order autocorrelation function that accounts for diffusion and antibunching in a system of single emitters (no clustering) is[25]

$$g^{(2)}(\tau) = 1 + \frac{1}{N(1+\tau/\tau_D)} - \frac{1}{N}e^{-(W+\Gamma)\tau} \quad (2)$$

Here, the first term (equal to 1) accounts for the Poissonian background of the measurement due to random diffusion of

chromophores within the focal volume. The second term accounts for diffusion of emissive particles through the focal volume, where N is the average particle number in this volume (average occupation factor) and τ_D is the average particle diffusion time. The final term arises from photon antibunching, which is due to the quantum nature of the NQD emitters; here, W is the pump rate, and Γ is the radiative rate.

The solid lines in Figure 2a depict the general form of the correlation function for the situation where a sample is composed of well-isolated chromophores (no clustering). In this case, the amplitudes of the short time ("antibunching dip") and long time (decay due to diffusion) components are the same and equal to $1/N$. For example, if an excitation volume contains two isolated NQDs ($N = 2$) the amplitude of the correlation signal is 1.5 for correlation times longer than the radiative lifetime and shorter than the diffusion time while the amplitudes of both the antibunching dip and the diffusion component are 1.

When more than one chromophore is associated with each diffusing particle, the drop in the correlation signal at $t = 0$ no longer matches signal decay at long times because of an increased probability of detecting two photons with zero delay. This effect leads to a reduced antibunching dip. For the case where each diffusing particle is composed of n chromophores, the second order autocorrelation function is given by

$$g^{(2)}(\tau) = 1 + \frac{1}{N(1+\tau/\tau_D)} - \frac{1}{Nn}e^{-(W+\Gamma)\tau} \qquad (3)$$

For $n > 1$, this expression yields the antibunching signal and the diffusion component that have different amplitudes. Specifically, the long-time decay component is still $1/N$, while the depth of the antibunching dip reduces to $1/(Nn)$ (dashed line in Figure 2a). For example, for a sample with $N = 2$ that is composed of particles with 2 chromophores ($n = 2$), $g^{(2)}(0)$ is 1.25, while the signal amplitude is still 1.5 as in the case without aggregation.

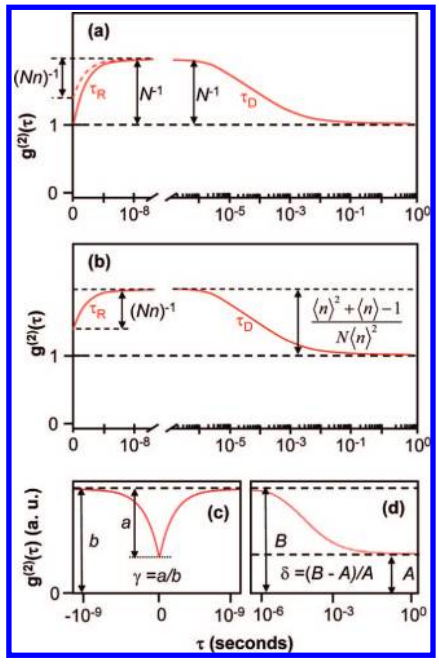

Figure 2. An approximate shape of the second-order intensity autocorrelation function $g^{(2)}$ on time scales relevant to radaitive decay (short times) and diffusion (long times) for single quantum emitters (solid line in panel a), clusters containing a fixed number (n) of emitters (dashed line in panel a), and the situation where the number of emitters per cluster is distributed according to Poisson statistics (b); N is the number of particles diffusing within the detection volume. The relation between the quantities measured in antibunching measurements (c) and FCS (d) and the normalized depth of the antibunching dip (γ) and the long-time decay amplitude (δ) related to diffusion.

A further extension of this model is required to account for the fact that in real samples there is a distribution of cluster sizes. To incorporate this distribution in the model, one can use the approach from ref 25, where the number of chromophores per particle, n, are weighted according to probabilities $p(n)$. The new expression that accounts for dispersion in the cluster sizes is

$$g^{(2)}(\tau) = 1 + \frac{\sum_{m=0}^{\infty} p(m)(m+1)^2}{N\left(\sum_{m=0}^{\infty} p(m)(m+1)\right)^2}\frac{1}{1+\tau/\tau_D} - \frac{1}{N\sum_{m=0}^{\infty} p(m)(m+1)}e^{-(W+\Gamma)\tau} \qquad (4)$$

where $m = n - 1 = 0, 1, 2$ is the number of emitters in a cluster in excess of 1. Given that most of the NQD solutions studied here are in the highly dilute limit, we can describe the distribution of cluster sizes by Poisson statistics observed previously, for example, in aggregated NC bioconjugates[26]

$$p(m) = \frac{\langle m\rangle^m}{m!}e^{-\langle m\rangle} \qquad (5)$$

where $\langle m\rangle$ is the average value of m in the sample. Combining eqs 4 and 5, we obtain

$$g^{(2)}(\tau) = 1 + \frac{\langle n\rangle^2 + \langle n\rangle - 1}{N\langle n\rangle^2}\frac{1}{1+\tau/\tau_D} - \frac{1}{N\langle n\rangle}e^{-(W+\Gamma)\tau} \qquad (6)$$

where $\langle n\rangle = \langle m\rangle + 1$ is the average cluster size (clustering parameter). Figure 2b illustrates the shape of the correlation function given by eq 6. The long time decay of correlation function has a value of $\delta = (\langle n\rangle^2 + \langle n\rangle - 1)/(N\langle n\rangle^2)$, while the antibunching dip amplitude is $\Delta = 1/(N\langle n\rangle)$.

To determine $\langle n\rangle$ from photon correlation data, we analyze the behavior of $g^{(2)}$ on short and long time scales using antibunching and FCS measurements, respectively. The antibunching amplitude, a, at time zero is normalized by the asymptotic value, b, which yields $\gamma = a/b$ (Figure 2c). Using eq 6, we obtain $\gamma = \Delta/(1 + \delta)$. The short time amplitude, B, and the long-time background, A, of the FCS signal can be used to directly calculate the value of the diffusion-decay component as $\delta = (B - A)/A$ (Figure 2d). In our analysis, we normalize the acquired curves in such a way that $A = 1$; in this case, $\delta = B - 1$. Using the above expressions, which relate Δ and δ to N and $\langle n\rangle$, we can obtain the quadratic equation, the positive root of which yields $\langle n\rangle$ as function of the measured values of Δ and δ

$$\langle n\rangle = \frac{-\gamma + \delta + \gamma\delta + \sqrt{\delta^2 - 2\gamma\delta(1+\delta) + 5\gamma^2(1+\delta)^2}}{2\gamma(1+\delta)} \qquad (7)$$

We can further derive N from $N = 1/(\Delta\langle n\rangle)$.

3. Experimental Results and Discussion

Control Experiments: Application to Dye Molecules. A first set of photon correlation experiments was performed using the standard laser dye R590 in water. The purpose of these

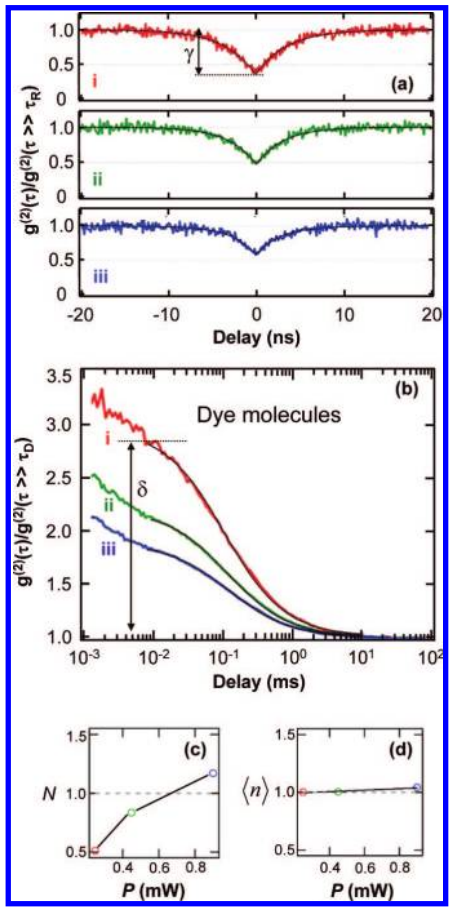

Figure 3. Pump-power-dependent antibunching (a) and FCS (b) curves from Rhodamine 590 molecules in water at excitation intensities of 250 μW (i), 450 μW (ii), and 900 μW (iii). Fits in panel b are truncated to include only the decay of $g^{(2)}$ due to diffusion. The initial faster decay, which ends near 10 μs, results from the buildup of the triplet population.[33] The values of N and $\langle n \rangle$ derived from data in panels a and b are shown as a function of excitation power, P, in panels c and d, respectively.

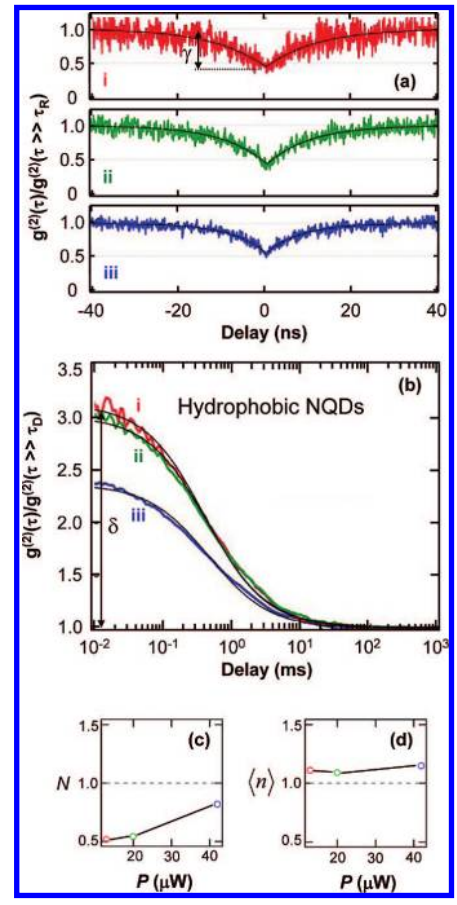

Figure 4. Pump-power-dependent antibunching (a) and FCS (b) curves from hydrophobic octylamine-capped NQDs in toluene recorded using pump intensities of 13 μW (i), 20 μW (ii), and 45 μW (iii). The values of N and $\langle n \rangle$ derived from data in panels a and b are shown as a function of excitation power in panels c and d, respectively.

studies was to test the validity of the proposed method for studies of aggregation. Since dye molecules do not have a propensity to aggregate, the expected value of n in this case is 1.

Figure 3a shows data from three antibunching measurements at different excitation powers ranging from 250 μW (i) to 900 μW (iii). These measurements are conducted on a dilute sample ($\sim$100 pM), for which less than one dye molecule is on average present in the detection volume. We observe that the antibunching amplitude, γ, decreases with increasing pump intensity from 0.66 to 0.43. Correspondingly, the long time amplitude, δ, in Figure 2b mirrors this decrease by going from 1.96 to 0.89. This trend is consistent with previous studies[27] and occurs because of intensity broadening of the excitation volume as a result of saturation of the excited-state transition in the molecules residing in the center of this volume. This effect leads to the effective increase in the number of particles, N, probed in correlation studies (occupation factor) and the respective decrease in the amplitude of the anticorrelation dip (Figure 3a), accompanied by the decrease of diffusion-related decay at long times (Figure 3b).

For the lowest intensity, the long-time decay amplitude is 1.96 that in conjunction with the antibunching amplitude $\gamma = 0.661$ yields $\langle n \rangle$ of 1.00 and N of 0.51. The increase in the pump intensity leads to an appreciable increase in N from 0.51 to 1.17 (Figure 3c) in going from trace i to iii in panels a and b of Figure 3. On the other hand, the corresponding values of $\langle n \rangle$ calculated from eq 7 (Figure 3d) still remain close to 1 (the observed deviation from 1 is less than 5%). These results indicate that the increase in the amplitude of the long-time FCS decay occurs not because of aggregation but rather because of effective expansion of the excitation volume as discussed above. These finding confirm the behavior expected for dye molecules (absence of aggregation) and indicate the feasibility of quantitative studies of clustering via combination of FCS and antibunching measurements.

Clustering in NQD Solutions: Hydrophobic Dots. Trace i in Figure 4a shows an antibunching curve taken at low pump intensity (13 μW) for core/shell CdSe NQDs in toluene. The pump intensities used in these measurements are more than an order of magnitude lower than those in studies of dyes to avoid formation of doubly excited NQDs (i.e., biexcitons). The generation of biexcitons reduces the amplitude of the antibunching dip,[28] that is, produces the same signature as formation of nanocrystal clusters. Therefore, in present experiments that focus on quantitative studies of aggregation, it is important to make sure that NQDs are excited in the single-exciton regime.

The antibunching dip in Figure 4a has an amplitude of 0.556. Combined with the long-time decay amplitude of 2.1, it yields $\langle n \rangle = 1.11$. This result suggests that the solution under investigation contains primarily isolated NQD emitters and further indicates the lack of any significant aggregation.

Traces ii and iii in panels a and b of Figures 4 were taken using higher excitation intensities of 20 and 42 μW, respectively. As intensity increases, a prominent qualitative change is a decrease in the antibunching amplitude that is echoed in the

long time traces by a decrease in the diffusion-related component. Despite these changes that indicate an increase in N (Figure 4c), the number of dots per diffusing particle calculated for each excitation level is close to 1 ($\langle n \rangle = 1.11$, 1.09, and 1.15 from the lowest to the highest pump intensity; see Figure 4d). This result shows that the observed changes in autocorrelation traces are not due to photoinduced formation of dot aggregates but rather due to an effective increase in the excitation volume, as in the case of dye molecules in Figure 3.

The uniformity of the clustering parameter under these excitation conditions also suggests that the effect of luminescence intermittency or "blinking" observed in single-dot studies of solid-state samples[16,29] likely does not significantly affect the correlation results for solution-based samples. If blinking were a strong factor, it would manifest itself as an effective increase in the number of particles diffusing in the detection volume (parameter N). This effect would reduce the long-time decay amplitude of $g^{(2)}$ and, hence, affect the clustering parameter derived from the correlation traces. Further, since blinking typically becomes stronger with increasing intensity, the values of $\langle n \rangle$ would also exhibit pump-intensity dependence. Since we do not detect any appreciable changes in $\langle n \rangle$ in response to changes in the pump intensity, it implies that the effects of blinking on time scales characteristic of NQD diffusion in the detection volume are negligible. The fact that blinking has a minimal effect on FCS traces was also pointed out in previous reports by Larson et al.[13] and Yao et al.[30] Furthermore, Yao et al.[30] directly showed that the "on-off-on" blinking events within the probed volume on the diffusion-related time scale (on the order of 1 ms in these experiments) were quite rare. In our experiments, this type of blinking event is even more unlikely because our excitation powers are at least an order of magnitude lower compared to those used in ref 30.

The near unity values of $\langle n \rangle$ indicate that most of the NQDs (~90%) in our toluene-based samples are present in the form of isolated particles. The low degree of dot clustering observed in these samples is not always seen for samples prepared with organic solvents. In fact, the degree of clustering represents a complex dependence on NQD surface passivation, the identity of the solvent, and the conditions of storage. For example, measurements on the sample in Figure 4 conducted a few weeks later indicated a higher degree of clustering ($\langle n \rangle > 1.5$) than in a freshly prepared solution ($\langle n \rangle < 1.2$). Interestingly, the measurements on a new NQD dilution prepared from a high-concentration growth solution aged for the same time showed a near unity clustering parameter. Since NQDs with partial passivation are typically more prone to aggregation than well-passivated nanocrystals, these findings imply that the use of more concentrated solutions slows down the loss of surface passivation. This behavior is expected given the widely accepted picture of dynamic equilibrium between free ligands in solution and those coordinated to NQD surfaces.[31]

Clustering in NQD Solutions: Hydrophilic Dots. In addition to standard hydrophobic NQDs, we have also studied hydrophilic biotinylated CdSe dots (purchased from Invitrogen). In comparison to standard NQDs, which have extended alkyl chains as their outermost passivation layer, water-soluble NQDs have a "polymeric" shell with a variety of different solubilizing groups. This polymeric shell is roughly fixed, i.e., there is little to no equilibration with solvent, while for standard NQDs the labile passivating ligands are in dynamic equilibrium with unbound ligands in the solvent. The "robustness" of the polymeric shell surrounding water-soluble dots allows one to maintain large emission quantum yields even at high degrees of dilution. In contrast, standard NQDs show a rapid drop in the PL efficiency at high dilution factors as a result of the loss of surface passivation.

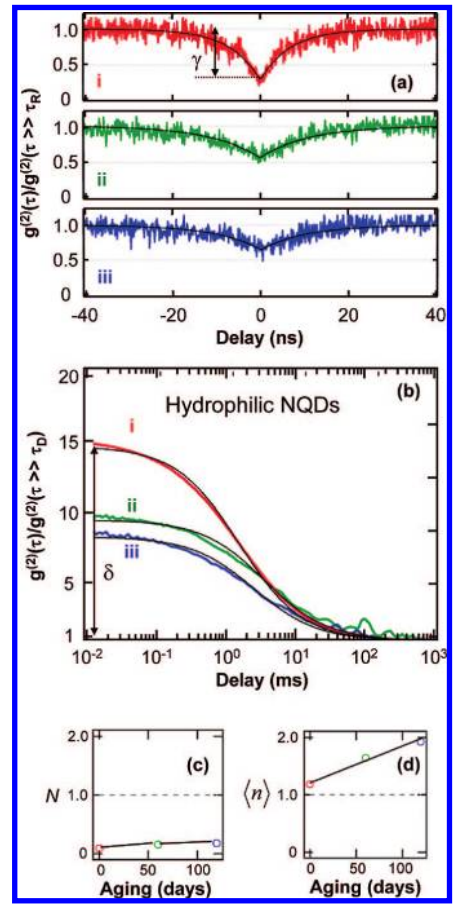

Figure 5. The antibunching (a) and FCS (b) curves from hydrophilic biotinylated NQDs in water as a function of sample aging recorded for a freshly prepared solution (i) and for the same sample but for 60 (ii) and 120 days (iii) following the preparation (pump intensity is 15 μW). The values of N (c) and $\langle n \rangle$ (d) derived from data in panels a and b are shown as a function of sample aging in panels c and d, respectively.

High-emission efficiencies attainable with dilute biotinylated samples allowed us to experimentally realize the regime of very low occupation factors of the detection volume with $N \ll 1$. In this situation, the quantum nature of NQD emitters becomes particularly pronounced, as manifested, e.g., in the increased amplitude of the antibunching signal. For example, based on autocorrelation traces recorded for a freshly prepared dilute sample of water-soluble dots (see curve i in panels a and b of Figures 5), $\langle n \rangle$ is 1.18 while N is less than 0.1. Because of the small value of the occupation factor, the antibunching dip becomes very pronounced and its amplitude reaches the value of more than 0.7, which exceeds typical values obtained with standard hydrophobic NQDs. In Figure 5, we also attempt to evaluate the effect of aging on the degree of aggregation of water-soluble dots. Specifically, in addition to autorrelation data for a fresh sample (trace i in panels a and b), we show traces measured for the same sample aged for 60 and 120 days (traces ii and iii, respectively). As indicated above, the clustering parameter for the fresh sample is 1.18 and is comparable to that measured for hydrophobic NQDs (Figure 4d). This result indicates that freshly prepared aqueous solutions of biotinylated NQDs do not have a significant amount of dot aggregates. On the other hand, for samples aged for 60 and 120

days the values of $\langle n \rangle$ are 1.5 and 1.95, respectively (Figure 5d), indicating a gradual increase in the degree of aggregation. Assuming a Poissonian distribution of cluster sizes, we obtain that for a freshly prepared sample, the ratio of the concentrations of single dots and double-dot clusters is greater than 4, while it decreases to ca. 1 for the sample aged for 120 days. Aging-dependent clustering in hydrophilic NQD samples have been previously observed in several reported studies including, for example, ref 32.

4. Conclusions

We have performed FCS and antibunching studies of solutions of CdSe NQDs. Direct measurement of autocorrelation traces on time scales of NQD diffusion and the radiative decay yield information on the number of NQDs per diffusing cluster (clustering parameter) as well as the number of the emitting particle in the detection volume (occupation factor). Using these measurements, we can reliably establish the regime when only one dot or less is present in the detection volume, which can, in principle, allow single-dot sensitivity in spectroscopic studies of solution samples.

We apply the combination of FCS and antibunching measurements for quantifying the degree of aggregation in toluene- and water-based NQD samples. We first validate this method by conducting correlation studies of dilute solutions of Rh590 in water that indicate the expected value of 1 for the clustering parameter $\langle n \rangle$ (determined with better than 5% accuracy). We further analyze the degree of aggregation for NQDs in both an organic solvent (toluene) and water. We observe that freshly prepared solutions show near-unity values of $\langle n \rangle$ indicating that dots are mostly present in the form of well-isolated particles. The degree of aggregation increases as samples are aged. For example, in water-soluble biotinylated samples aged for 120 days the number of two-dot aggregates becomes approximately equal to the number of isolated NQDs.

Previously, clustering in NQD samples has been analyzed using dynamic light scattering (DLS),[32] which is a technique especially useful in studies of larger-size aggregates. The method reported in the present paper is complimentary to DLS as it provides extremely high sensitivity in studies of weakly aggregated samples in the regime of near-unity clustering parameter. Understanding this regime is important from the prospective of both bioimaging and biolabeling. Specifically, the formation of even small clusters can significantly alter NQD interactions with cells and organelles. Further, clustering may complicate tracking or optical correlation studies of binding events that rely on single-NQD detection.

The ability to study single dots in solution opens interesting opportunities in both biorelated research and also in studies of fundamental photophysics of nanocrystals. One attractive possibility is single-dot studies of the effects of environment on light-emitting properties of nanocrystals. Further, single-dot studies of multiexciton behaviors normally conducted at high excitation powers could benefit from a higher photostability of solution samples compared to that of submonolayer films traditionally used in such studies. Other interesting research directions may involve studies of energy-transfer phenomena in single donor−acceptor NQD pairs and complex electronic interactions in hybrid nanostructures comprising NQDs and, e.g., dyes, polymers, or nanoscale metals.

Acknowledgment. We thank Peter Goodwin and Jim Werner for insightful discussions and technical advice. This work was supported by the Office of Science of the U.S. Department of Energy (DOE) and Los Alamos LDRD funds. Photon correlation measurements were conducted at the DOE Center for Integrated Nanotechnologies (CINT) jointly operated by Los Alamos and Sandia National Laboratories as part of the CINT user program. D.A.B. acknowledges financial support through the CINT Distinguished Postdoctoral Fellowship Program.

References and Notes

(1) Klimov, V. I.; Ivanov, S. A.; Nanda, J.; Achermann, M.; Bezel, I.; McGuire, J. A.; Piryatinski, A. *Nature* **2007**, *447*, 441–446.
(2) Klimov, V. I.; Mikhailovsky, A. A.; Xu, S.; Malko, A.; Hollingsworth, J. A.; Leatherdale, C. A.; Eisler, H. J.; Bawendi, M. G. *Science* **2000**, *290*, 314–317.
(3) Coe, S.; Woo, W.-K.; Bawendi, M. G.; Bulovic, V. *Nature* **2002**, *420*, 800–803.
(4) Colvin, V. L.; Schlamp, M. C.; Alivisatos, A. P. *Nature* **1994**, *370*, 354–356.
(5) Alivisatos, P. *Nat. Biotechnol.* **2004**, *22*, 47–52.
(6) Bruchez, M.; Moronne, M.; Gin, P.; Weiss, S.; Alivisatos, A. P. *Science* **1998**, *281*, 2013–2015.
(7) Dubertret, B.; Skourides, P.; Norris, D. J.; Noireaux, V.; Brivanlou, A. H.; Libchaber, A. *Science* **2002**, *298*, 1759–1762.
(8) Hines, M. A.; Guyot-Sionnest, P. *J. Phys. Chem.* **1996**, *100*, 468–471.
(9) Murray, C. B.; Norris, D. J.; Bawendi, M. G. *J. Am. Chem. Soc.* **1993**, *115*, 8706–8715.
(10) Peng, Z. A.; Peng, X. G. *J. Am. Chem. Soc.* **2001**, *123*, 183–184.
(11) Klimov, V. I. *Semiconductor and Metal Nanocrystals: Synthesis and Electronic and Optical Properties*; Marcel Dekker: New York, 2004.
(12) Chan, W. C. W.; Nie, S. M. *Science* **1998**, *281*, 2016–2018.
(13) Larson, D. R.; Zipfel, W. R.; Williams, R. M.; Clark, S. W.; Bruchez, M. P.; Wise, F. W.; Webb, W. W. *Science* **2003**, *300*, 1434–1436.
(14) Empedocles, S. A.; Norris, D. J.; Bawendi, M. G. *Phys. Rev. Lett.* **1996**, *77*, 3873–3876.
(15) Fomenko, V.; Nesbitt, D. J. *Nanolett.* **2008**, *8*, 287–293.
(16) Kuno, M.; Fromm, D. P.; Hamann, H. F.; Gallagher, A.; Nesbitt, D. J. *J. Chem. Phys.* **2000**, *112*, 3117–3120.
(17) Ebenstein, Y.; Mokari, T.; Banin, U. *Appl. Phys. Lett.* **2002**, *80*, 4033–4035.
(18) Doose, S.; Tsay, J. M.; Pinaud, F.; Weiss, S. *Anal. Chem.* **2005**, *77*, 2235–2242.
(19) Magde, D.; Elson, E. L.; Webb, W. W. *Biopolymers* **1974**, *13*, 29–61.
(20) Rochira, J. A.; Gudheti, M. V.; Gould, T. J.; Laughlin, R. R.; Nadeau, J. L.; Hess, S. T. *J. Phys. Chem. C* **2007**, *111*, 1695–1708.
(21) McHale, K.; Berglund, A. J.; Mabuchi, H. *Nanolett.* **2007**, *7*, 3535–3539.
(22) Sykora, J.; Kaiser, K.; Gregor, I.; Bonigk, W.; Schmalzing, G.; Enderlein, J. *J. Anal. Chem.* **2007**, *79*, 4040–4049.
(23) Chen, Y.; Vela, J.; Htoon, H.; Casson, J. L.; Werder, D. J.; Bussian, D. A.; Klimov, V. I.; Hollingsworth, J. A. *J. Am. Chem. Soc.* **2008**, *130*, 5026–5027.
(24) Felekyan, S.; Kuhnemuth, R.; Kudryavtsev, V.; Sandhagen, C.; Becker, W.; Seidel, C. A. M. *Rev. Sci. Instrum.* **2005**, *76*, 083104−083114.
(25) Mets, U. *Antibunching and Rotational Diffusion in FCS. In Fluorescence Correlation Spectroscopy: Theory and Applications*; Rigler, R. E., Ed.; Springer-Verlag: Berlin, 2001; Vol. 65, pp 346−359.
(26) Pons, T.; Medintz, I. L.; Wang, X.; English, D. S.; Mattoussi, H. *J. Am. Chem. Soc.* **2006**, *128*, 15324–15331.
(27) Mets, U.; Widengren, J.; Rigler, R. *Chem. Phys.* **1997**, *218*, 191–198.
(28) Fisher, B.; Caruge, J. M.; Zehnder, D.; Bawendi, M. *Phys. Rev. Lett.* **2005**, *94*, 087403−087404.
(29) Nirmal, M.; Dabbousi, B. O.; Bawendi, M. G.; Macklin, J. J.; Trautman, J. K.; Harris, T. D.; Brus, L. E. *Nature* **1996**, *383*, 802–804.
(30) Yao, J.; Larson, D. R.; Vishwasrao, H. D.; Zipfel, W. R.; Webb, W. W. *Proc. Natl. Acad. Sci.* **2005**, *102*, 14284–14289.
(31) Kalyuzhny, G.; Murray, R. W. *J. Phys. Chem. B* **2005**, *109*, 7012–7021.
(32) Pons, T.; Uyeda, H. T.; Medintz, I. L.; Mattoussi, H. *J. Phys. Chem. B* **2006**, *110*, 20308–20316.
(33) Widengren, J.; Mets, U.; Rigler, R. *J. Phys. Chem.* **1995**, *99*, 13368–13379.

JP806219S